Bull. Astr. Soc. India (2002) 30, 767–772

Ejection of quasars from galaxies and the variable mass hypothesis

Prashanta Kumar Das

Indian Institute of Astrophysics, Koramangala, Bangalore 560034, India

Abstract. The present work investigates the dynamics of ejection of quasars from galaxies in the Variable Mass Hypothesis (VMH), originally discussed by Narlikar & Das to provide a theoretical interpretation of the observed alignments of quasars with active galaxies. According to the VMH a typical quasar is ejected from the parent galaxy with zero rest mass which grows with time through a Machian interaction whereas its speed decreases from its initial value which equals the speed of light. A consistent picture emerges from the calculations, based on the recent observational data from X-ray astronomy, in which the quasar passes through a continuous sequence of decreasing redshifts and increasing masses as it grows old. The calculations also provide a method for distinguishing between quasars which can escape the gravitational influence of the parent galaxies and the ones which are bound.

1. Introduction

The dynamics of ejection of X-ray quasars from galactic nuclei is studied in terms of a model, originally developed by Narlikar and Das (ND, 1980), which is based on the Variable Mass Hypothesis [VMH] of the conformal gravitation theory of Hoyle and Narlikar (HN, 1966). An attempt has been made to quantitatively relate the observed ordering of the redshifts of ejected quasars with their separations from the galaxy, intrinsic redshifts and ages.

2. Narlikar-Das model

The Machian HN theory admits solutions in which the particle masses can vary with space and time [VMH]. In the ND scenario in an Einstein-deSitter universe [$k = 0$, $q_0 = 1/2$] the bulk of the matter is assumed to be "normal" [constant particle masses] but a quasar Q "born" in the nucleus of a galaxy G at an epoch $t_Q > 0$ is shown to have vairable particle masses given by

$$m(t) = m_o\,[1-(\frac{t_Q}{t})^{1/3}]^2,\ m_o = \text{constant} \tag{1}$$

and its redshift is given by

$$(1 + z_Q) = \frac{t_o^{2/3}}{t^{2/3}} \quad \frac{1}{[1 - (\frac{t_Q}{t})^{1/3}]^2}$$

$$= (1 + z_G) \times (1 + z_a),\ t_o = \text{present epoch} \tag{2}$$

which shows that z_Q has an "anomalous" redshift component z_a and $z_Q > z_G$.

Thus Q is born as a massless object at $t = t_Q$ in G and its mass grows while its redshift decreases with the passage of time. Narlikar and Das obtained the following equations of motion for such a variable mass quasar Q, rejected radially outwards from the nucleus of a galaxy G of mass M, in the Schwarzchild field of G at an epoch $t = t_Q$:-

$$x = \frac{\dot{R}}{(1 - \frac{2M}{R})}$$

$$\dot{x} + (1 - x^2) \left[\frac{M}{R^2} + \frac{2t_Q^{1/3}}{3t(t^{1/3} - t_Q^{1/3})} \left\{x - \frac{2R\ (1 - \frac{2M}{R})}{3t}\right\} + \frac{2}{9}\frac{R}{t^2}\left\{1 - \frac{2Rx}{t(1 - \frac{2M}{R})}\right\}\right] = 0 \tag{3}$$

These equations were numerically solved. The main results of the numerical computations may be summarized as follows :-

(i) Q, though fired with the speed of light at $t = t_Q$ since it is massless, quickly slows down as its mass grows.

(ii) The motion of Q is characterized by a parameter η_o which determines the time span of relativistic motion. For a given pair of G and Q there exists an η_c such that :

For $\eta_o < \eta_c$, Q forms a bound system with G undergoing damped oscillations of decreasing periods.

For $\eta_e > \eta_c$, Q remains unbound till the epoch of observation $t = t_G$.

Thus η_c is analogous to "escape speed".

(iii) The maximum separation $R_{max}(\eta_c)$ between a bound quasar Q and galaxy G decreases very slowly with z_G and z_Q and is of the order of 300 ~ 400 kpc for typical Q – G associations.

The ND model, developed specifically to interpret the anomalous redshifts of quasars, can adequately explain the observed features of typical quasar-galaxy associations such as

(i) The well known angular separation $\theta_{QG} \propto \frac{1}{z_G}$ relation which follows from the near constancy of $R_{max}(\eta_c)$.

(ii) Alignments and redshift bunchings, e.g. the Arp-Hazard triplet pair (Arp and Hazard, 1980).

(iii) Apparent luminous connections between high-z quasars and low-z galaxies such as 3C232 (z = 0.534) and NGC 3067 (z = 0.005) (Das, 1993).

3. Application of new Q-G systems

Recent findings by Arp and others (Arp, 1998) include many new examples from X-ray astronomy. The present work examines how well the Narlikar-Das scenario stands up to these recent data. The following systems have been studied. (Narlikar et al., 2002).

(i) The galaxy NGC 3516 with tife quasars, (ii) The galaxy NGC 4258 with two quasars, (iii) The galaxy NGC 5985 with six quasars, (iv) The galaxy IC 4553 [Arp 220] with four companions.

The following numerical procedure is adopted :-

The equations of motion for Q (eq. 3) are numerically solved with increasing values of the parameter η_o till the critical η_c is reached. If the calculated $R_{max}(\eta_c)$ is greater than the observed Q-G separation we classify Q as a bound quasar. Otherwise we conclude that Q is unbound at least till the epoch of observation $t = t_G$. The value of η_o which yields the observed separation is also calculated.

The results of the computations are shown in Tables 1–4. Thus it is seen that for the cases (i), (ii) and (iv) all the quasars are bound whereas for NGC 5985 the model predicts some unbound quasars. Also the Doppler component of the spectral shift in the quasars is very small (10 - 400 km/sec) in this scenario. Figure 1 shows that the maximum separation $R_{max}(\eta_c)$ slowly decreases as the quasar redshift increases. Figure 2 illustrates that the higher redshift quasars are younger. The variation of the ejection and escape velocities, estimated in terms of he η parameter, with the quasar redshift is shown in figure 3.

Table 1. NGC 3516 : Redshift(z_G) = 0.009, $M = 3 \times 10^{10} M_\odot$, $\theta_G = 1.8'$.

Object	Redshift (z_Q)	Radial separation (kpc)	$\eta_c \times 10^6$	$\eta_o \times 10^6$	Velocity at T_G +ve outward -ve inward (km/s)	Status : Bound / Unbound
Q1107+7232	2.1	94.84	6.84	5.95	–32.3	B
Q1105+7238	1.4	162.15	5.08	4.66	–16.1	B
Q1105+7242	0.93	240.17	3.45	3.35	–5.2	B
Q1106+7244	0.69	226.62	2.45	2.36	–7.8	B
Q1108+7226	0.33	245.42	0.80	0.77	–6.8	B

Table 2. NGC 4258 : Redshift(z_G) = 0.002, $M = 7.5 \times 10^{10} M_\odot$, $\theta_G = 4.5'$.

Object	Redshift (z_Q)	Radial separation (kpc)	$\eta_c \times 10^6$	$\eta_o \times 10^6$	Velocity at T_G +ve outward -ve inward (km/s)	Status : Bound / Unbound
X-ray	0.40	42.28	1.79	1.64	−111.8	B
X-ray	0.65	47.68	3.38	3.05	−102.9	B

Table 3. NGC 5985 (Sey1) : Redshift(z_G) = 0.008, $M = 7.5 \times 10^{10} M_\odot$, $\theta_G = 1.25'$.

Object	Redshift (z_Q)	Radial separation (kpc)	$\eta_c \times 10^6$	$\eta_o \times 10^6$	Velocity at T_G +ve outward -ve inward (km/s)	Status : Bound / Unbound
HS1543+5921	0.807	718.05	4.21	5.18	27.7	U
RXJ15509+5856	0.348	1759.11	1.39	2.90	86.7	U
SBS1537+595	2.125	233.51	9.55	8.77	−17.3	B
SBS1535+596	1.968	490.37	9.10	10.20	13.1	U
SBS1533+588	1.895	1056.63	8.88	16.66	50.3	U
SBS1532+598	0.69	937.93	3.53	4.98	41.6	U

Table 4. Arp 220 (IC 4553) Redshift(z_G) = 0.018, $M = 10^{13} M_\odot$, $\theta_G = 0.75'$.

Object	Redshift (z_Q)	Radial separation (kpc)	$\eta_c \times 10^6$	$\eta_o \times 10^6$	Velocity at T_G +ve outward -ve inward (km/s)	Status : Bound / Unbound
Arp No.2 (RSO)	1.26	301.44	32.98	29.08	−448.7	B
Arp No.9 (BSO)	1.25	344.5	32.75	28.93	−408.9	B
20.N	0.23	1283.27	3.67	3.52	−110.7	B
20.3S	0.46	1856.0	10.75	10.59	−22.7	B

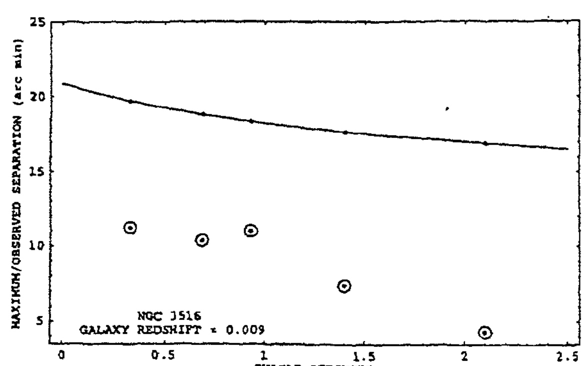

Figure 1. This shows that the maximum separation between the quasar and galaxy decreases as the quasar redshift increases. The observed points are shown by open circles.

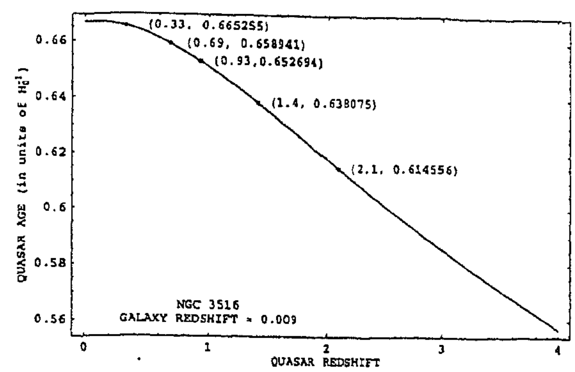

Figure 2. Quasar age against its redshift: the larger redshift quasars are younger.

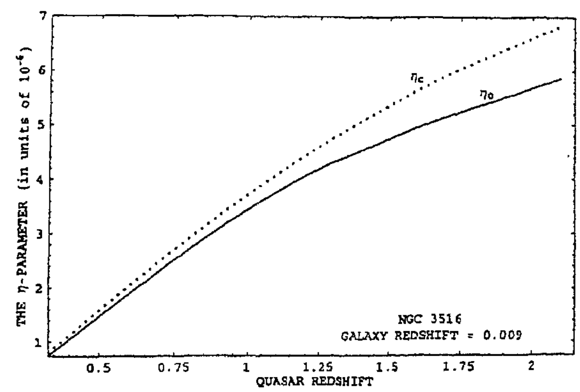

Figure 3. The escape velocities of the quasars diminish as their intrinsic redshifts get smaller. The above figure uses the parameter η_0, which indicates the time scale over which the ejected motion is relativistic. Thus the larger the value of this parameter, the faster is the outward motion of the ejecta, with η_c corresponding to the escape speed. The dotted line shows the value η_c while the continuous line shows the value η_0 for actual observations.

4. Conclusions

A consistent picture emerges from these calculations in which a typical quasar starts its life as a young lump of matter ejected from the parent galaxy with the speed of light and zero rest mass. As its mass grows with age the quasar passes through a continuous sequence of decreasing redshifts. Whether the quasar will eventually escape from the gravitational influence of the galaxy depends upon the initial energy of ejection, measured in terms of the parameter η_0. It is possible that some of the quasars seen in isolation are such "escaped" quasars. On the other hand the bound quasars move in steadily shrinking orbits around the parent galaxy.

This work is entirely based on classical mechanics, modified by the Machian theory of gravity. In order to understand the puzzling phenomenon of redshift periodicities (quantization) in quasar redshift distribution [for references see Narikar et al., 2002 (op. cit.)] a quantum version of the present formalism, in which the mass and hence the redshift are quantized, is needed. Work is in progress to quantify this idea.

References

Arp H.C., Hazard C., 1980, Ap.J., 240, 726.
Arp H.C., 1998, Seeing Red, Apeiron, Montreal.
Das P.K., 1993, Proc. 6th IAU Asian Pacific Regional Meeting, Pune.
Hoyle F., Narlikar J.V., 1966, Proc. Roy. Soc. A. 294, 138.
Narlikar J.V., Das P.K., 1980, Ap. J. 240, 401.
Narlikar J.V., Vishwakarma R.G., Banerjee S.K., Das P.K., Arp H.C., 2002, Int. J. Mathematical Phys., [D], (in press).